Hemocyte morphology and phagocytic activity in the common cuttlefish (Sepia officinalis).

Charles Le Pabic, Didier Goux, Maryline Guillamin, Georges Safi, Jean-Marc Lebel, Noussithé Kouéta, Antoine Serpentini

Hemocyte morphology and phagocytic activity in the common cuttlefish (*Sepia officinalis*)

Charles Le Pabic[a,b,c]*, Didier Goux[a,d], Maryline Guillamin[a,e], Georges Safi[a,b,c], Jean-Marc Lebel[a,b,c], Noussithé Koueta[a,b,c], Antoine Serpentini[a,b,c]

[a] Normandie Université, F-14032 Caen, France

[b] UMR BOREA, MNHN, UPMC, UCBN, CNRS-7028, IRD-207, IBFA Université de Caen Basse-Normandie, Esplanade de la Paix, CS 14032, 14032 Caen cedex, France

[c] Centre de Recherches en Environnement Côtier, Université de Caen Basse-Normandie, 54 rue du Docteur Charcot, 14530 Luc-sur-Mer, France

[d] CMAbio, Université de Caen Basse-Normandie, F-14032 Caen cedex, France

[e] Plateau de cytométrie SFR ICORE, Université de Caen Basse-Normandie, F-14032 Caen cedex, France

*Corresponding author: Charles Le Pabic
UMR BOREA, MNHN, UPMC, UCBN, CNRS-7028, IRD-207, IBFA Université de Caen Basse-Normandie, Esplanade de la Paix, CS 14032, 14032 Caen cedex, France
Tel.: (+33) 231 565 102
Fax: (+33) 231 565 346
e-mail : charles.lepabic@gmx.fr

1. Introduction

Invertebrates resist pathogens despite their lack of adaptive immunity [1]. The tremendous variety of invertebrate life histories and ecological niches suggests a great diversity of immune strategies [2]. Among Mollusca – one of the most diverse groups of animals [3], studies of immunity have mostly focused on bivalves (e.g. [4–14]) and gastropods (e.g. [15–20]), while few studies have focused on cephalopods [21,22]. Cephalopods are an interesting model because of their (1) vertebrate-like high-pressure closed circulatory system, (2) high sensitivity to environmental parameters, (3) short-life span and (4) elevated metabolic rate [23,24]. Moreover, their economical importance has recently grown in terms of fisheries and aquaculture (e.g. [25–29]).

As in other invertebrates, the cephalopod immune system relies on humoral factors and cell-mediated mechanisms acting together to eliminate invading micro-organisms [30,31]. Humoral factors mainly include lectins (e.g. agglutinins, opsonins), antimicrobial factors (e.g. peptides, acid phosphatases, lysozymes), and several signaling pathways including prophenoloxidase (proPO) and proteolytic cascades [2,32]. In contrast, cell-mediated defense mechanisms are primarly performed by hemocytes (Hcs) – cells synthetized in white bodies and freely circulating in plasma and infiltrating in tissues [33,34]. Hcs are of central importance to invertebrates because of their involvement in numerous physiological functions [35–39], including their ability to phagocytose, encapsulate and destroy foreign particles [18,30,40]. In cephalopods, Hcs have mainly been described as a one cell-type population[1]

[1] **Abbreviations:** FCM: flow cytometry; Hc: hemocyte; Hcy: hemocyanin; MPS: molluscan physiological saline; NR: neutral red; PI: protease inhibitor; PO: phenoloxidase**;** proPO: prophenoloxidase; SEM: scanning electron microscopy; SD: standard deviation; TEM: transmission electron microscopy.

with large lobate nucleus and abundant granules, able to phagocytose [31,34,40–42]. However, these Hc descriptions were mainly performed in Octopodidae as well as in the sepiolidae *Euprymna scolopes* and little is known about the immune cellular factors of other cephalopod species such as the sepiidae (cuttlefish) *Sepia officinalis*. Because of the distinct ecology of Sepiidae within Cephalopodia [27,43,44], they may also have distinct immune requirements.

In this study, we performed cytological stainings, electron microscopy and flow cytometry (FCM) analysis to morphologically characterize *S*. *officinalis* Hcs. In addition, we investigated humoral factor localization between plasma and cells, and phagocytic reactions at several incubation times, temperatures and plasma concentrations. Our results highlighted one granulocyte population with various densities of acidophilic granules and unstained vesicles. The Hcs, which contained acid phosphatase, lysozyme and proPO system enzymes, had high phagocytic ability, modulated by plasma in our assay conditions.

2. Material and methods

2.1. Animals

Thirty-one adult cuttlefish *S. officinalis* (21.5 ± 3.1 cm mantle length) were obtained from traps deployed during spring 2011 and 2012 along the Calvados coast (Normandy, France). Cuttlefish were then conditioned at the Centre de Recherches en Environnement Côtier (Luc-sur-Mer, Normandy, France) in 4500-L tanks in an open seawater circuit for at least 2 days, fed with crustaceans *Crangon crangon* and *Carcinus maenas*, and starved for 1 day before experimentation. The sex of each individual was determined.

2.2. Hemolymph collection

Before hemolymph sampling and following ethical procedures (Directive 2010/63/EU), cuttlefish were anesthetized as described by Andrews et al. [45] through placement for 10 min in seawater containing 2% ethanol. Between 9 and 13 ml of hemolymph was then withdrawn from the anterior mantle vein [46] using a syringe with 18-gauge needle. The sample was transferred into a sterile tube, diluted or not with one volume of cooled sterile antiaggregative modified Alsever solution (115 mM glucose; 27 mM sodium citrate; 11.5 mM EDTA; 382 mM NaCl pH 7.5) [47], depending on the procedure (see below), and kept on ice to minimize cell clumping. Hc viability was checked by mixing one volume of Alsever-diluted hemolymph with one volume of trypan blue solution (0.4%) and Hc concentration was determined with non diluted hemolymph using a Thoma cell. Once sampling was completed, animals were euthanized by increasing ethanol concentration to 10% [48].

2.3. Chemicals

Sodium chloride (NaCl), anhydrous and hexahydrate magnesium chloride ($MgCl_2$ and $MgCl_2{\cdot}6H_2O$), calcium chloride ($CaCl_2$), bovin serum albumin (BSA), Bradford reagent,

trypsin TPCK (N-Tosyl-L-phenylalanine chloromethyl ketone), Nα-benzoyl-L-arginine 4-nitroanilide hydrochloride (BAPNA), *p*-nitrophenyl-phosphate, dimethyl sulfoxide (DMSO), trizma hydrochloride (Tris-HCl), trizma base, 3,4-dihydroxy-L-phenylalanine (L-DOPA), tropolone, hen egg white (HEW) lysozyme, freeze-dried *Micrococcus lysodeikticus*, sodium phosphate dibasic dihydrate ($Na_2HPO_4{\cdot}2H_2O$), citric acid ($C_6H_8O_7$), Wright stain, neutral red, L-15 medium (Leibovitz), potassium chloride (KCl), magnesium sulphate heptahydrate ($MgSO_4{\cdot}7H_2O$), formaldehyde solution, L-glutamine, streptomycin, sodium hydroxide (NaOH), ethylenediaminetetraacetic acid (EDTA), trypan blue solution, methanol and HEPES were obtained from Sigma-Aldrich (France). Halt Protease Inhibitor Cocktail, EDTA-Free (100X) was obtained from Thermo Fisher Scientific (Waltham, USA). Ethanol was obtained from Carlo erba (Milan, Italy). Hemacolor® staining kit was obtained from Merck Millipore (Darmstadt, Germany). Low melting point agar was obtained from Carl Roth (Lauterbourg, France). All chemicals used for electron microscopy i.e. glucose, sodium citrate, glutaraldehyde, sodium cacodylate, sucrose, osmium tetroxide (OsO_4), propylene oxide, araldite resin, uranyl acetate and lead citrate were obtained from Electron Microscopy Sciences (Hatfield, PA, USA).

2.4. Morphological characterization of S. officinalis Hcs

2.4.1. Hemolymph cell monolayer stainings

For Hc staining, one drop of hemolymph was placed on a Thermanox™ coverslip (Thermo Fisher Scientific, Waltham, USA) and allowed to adhere for 30 min at 15°C. Before staining, coverslips were rinsed in Molluscan Physiological Saline (MPS; 0.4 M NaCl, 0.1 M $MgSO_4$, 20 mM HEPES, 10 mM $CaCl_2$ and 10 mM KCl modified after [49]) to remove plasma. Hemacolor® staining was performed according to the manufacturer's recommendations. Wright staining was performed after 1 min air-drying by 1 min

dehydration in absolute methanol, following by 1 min in Wright solution (0.66% in methanol), then diluted (1:4) in distilled water during 4 min and rinsed. To highlight the cell lysosomal system, neutral red (NR) uptake was performed by incubating cells for 30 min in NR solution (1:500; NR stock solution (20 mg NR/ml DMSO):MPS) in a moist chamber at 15°C, before observation.

Freshly spread Hcs were observed using an inverted binocular microscope (Leica® DM IRB, Leica Microsystems, Wetzlar, Germany). Stained Hc observations were carried out with a Nikon Eclipse 80i light microscope with computer-assisted microscopic image analysis system, NIS-elements D 2.30 software (Nikon®, Champigny-sur-Marne, France).

2.4.2. Electron microscopy

After 10 min 300 × *g* centrifugation, Hc pellets (N = 5) were rinsed with MPS and fixed in 3.2% glutaraldehyde in 0.31 M sodium cacodylate buffer, with 0.25 M sucrose (pH 7.4) during for 90 min at 4°C. The cells were washed 3 times in rinsing solution (0.4 M sodium cacodylate, 0.3 M sucrose, pH 7.4). Then, cells were post-fixed 1 h with 1% OsO_4 in cacodylate buffer 0.2 M, with 0.36 M sucrose (pH 7.4) at 4°C (protected from light), and washed in rinsing solution.

For scanning electron microscopy (SEM), cells were sedimented for 7 days on Thermanox™ coverslip coated with poly-l-lysine (Thermo Fisher Scientific, Waltham, USA). They were then dehydrated in progressive bath of ethanol (70-100%) and critical point dried (Leica® EM CPD030). Finally, cells were sputtered with platinum and observed with scanning electron microscope JEOL 6400F. Freshly sampled cell diameters were determined by measuring 100 cells per cuttlefish (N = 5).

For transmission electron microscopy (TEM), cells were pellet in 2% low melting point agar at 40°C, and then dehydrated through increasing concentrations of ethanol (70-

100%) and propylene oxide 100%, embedded in araldite resine and allowed to polymerise for 48 h at 60°C. Ultrathin sections were done and contrasted with 2.5% uranyl acetate diluted in 50% ethanol for 30 min and contrasted for 5 min in Reynold's lead citrate [50]. Finally, cells were observed by transmission electron microscope JEOL 1011 and images were obtained with Camera Megaview 3 and Analysis Five software.

2.5. Biochemical analysis

2.5.1. Enzyme extraction

Hcs and plasma were separated in non diluted hemolymph by 500 × *g* centrifugation for 10 min at 4°C. Plasma was then removed, checked for absence of Hc microscopically, and stored in aliquots at -80°C until analysis. Upon complete plasma removal, Hc pellets were gently rinsed in either Tris buffer pH 7 (0.1 M Tris-HCl, 0.45 M NaCl, 26 mM $MgCl_2$ and 10 mM $CaCl_2$) for phenoloxidase (PO) assays [51] or Tris buffer pH 8 (10 mM Tris-HCl and 150 mM NaCl) for phosphatase, lysozyme and protease inhibitor (PI) assays [52]. Cells were resuspended at 10 × 10^6 cells ml^{-1} in same extraction buffer and sonicated at 60 W for 20 s. Cell extracts were then centrifuged at 10,000 × *g* and their supernatant aliquoted and stored at -80°C until analysis.

2.5.2. Enzymatic assays

All activities were expressed in relation to protein concentration measured by the Bradford method [53] using BSA as standard.

Total acid phosphatase activity was determined according to Moyano et al. [54] using *p*-nitrophenyl-phosphate 2% as substrate in a 1 M Tris buffer at pH 3. Then, 10 µl of supernatant was added to 10 µl of substrate in 96-well flat bottom plates (BD, USA). After 30 min incubation at 25°C, 100 µl of NaOH 1 M were added to stop the reaction. The

157 absorbance was measured at 405 nm using a Mithras LB 940 luminometer (Berthold, Thoiry,
158 France). Total acid phosphatase activity was expressed as specific activity (U mg^{-1} protein)
159 where one enzymatic unit corresponded to the absorbance recorded after incubation.
160 Lysozyme activity was quantified according to Malham et al. [55]. Fifty µl of HEW
161 lysozyme (85 µg ml^{-1} in Tris buffer pH 8 described in section *2.5.1.*) standard was serially
162 diluted in triplicate in 96-well flat bottom plates (BD, USA). Fifty µl of each sample was
163 added in triplicate to the 96-well plates as well as 50 µl of Tris buffer pH 8, as blanks. One
164 hundred and fifty µl of the substrate, freeze-dried *M. lysodeikticus* (75 mg/100 ml of
165 phosphate/citrate buffer pH 5.8 ($Na_2HPO_4 \cdot 2H_2O$, 4.45 g/250 ml distilled H_2O; citric acid
166 ($C_6H_8O_7$), 2.1 g/100 ml distilled H_2O; NaCl, 0.09 g/100 ml buffer)), was added to each well.
167 The reductions in turbidity in the wells were read on Mithras LB 940 luminometer (Berthold,
168 Thoiry, France) at 25°C for 5 minutes at 10 second intervals at 450 nm using negative
169 kinetics. Lysozyme concentrations were calculated from the standard curve (µg HEW
170 lysozyme equivalent ml^{-1}). Final lysozyme-like activity was thus expressed as µg HEW
171 lysozyme eq. mg $protein^{-1}$.
172 As described by Malham et al. [55] and Thompson et al. [56], PI activity was measured
173 by transferring 20 µl of sample and 10 µl of trypsin TPCK (100 µg ml^{-1} of 0.05 M Tris buffer
174 pH 8) in 96-well flat bottom plates (BD, USA), and mixed at room temperature for 5 minutes.
175 In parallel, intrinsic trypsin activity was measured by replacing 10 µl of trypsin by Tris buffer
176 pH 8 described above (section *2.5.1.*). A positive control was used by replacing the sample
177 with Tris buffer pH 8. Two hundred µl of BAPNA substrate solution (5.2 mg BAPNA ml^{-1}
178 DMSO) in 10 ml of 0.01 M trizma base buffer pH 7.4) was added to each well and incubated
179 for 15 minutes at room temperature. Absorbance was read at 405 nm using Mithras LB 940
180 luminometer (Berthold, Thoiry, France), and PI activity was expressed as the percentage of
181 trypsin sample inhibition (TI) compared to the positive control.

In order to partly discriminate PO synthesis and activation site, special care was taken to avoid unwanted activation of proPO during each step of the experiment. PO-like activity was measured spectrophotometrically by recording the formation of *o*-quinones, as described by Luna-Acosta [51] with slight modifications to distinguish artificially activated PO (APO) (corresponding to PO-like activity resulting from zymogenic PO (proPO) activation plus already 'active' form) and *in vivo* 'active' PO form [57]. PO assays were conducted in 96-well flat bottom plates (BD, USA). L-DOPA was used as substrate, at a final concentration of 10 mM [51] and prepared extemporaneously in Tris buffer pH 7 described above (section *2.5.1.*). Tropolone (10 mM) and trypsin TPCK (1 g l^{-1}) were used respectively as PO inhibitor and elicitor as previously described in *S. officinalis* [57,58]. To avoid uncontrolled proPO activation by intrinsic proteases, Halt Protease Inhibitor Cocktail, EDTA-Free (1X) wide spectrum PI was used. For each sample, autoxidation of sample, 'basal', 'inhibited' and 'activated' PO-like activities were measured. For non-enzymatic sample autoxidation, 10 µl of sample was mixed with Tris buffer pH 7. For 'basal' PO-like activity, 10 µl of sample was firstly mixed during 10 min with 1.4 µl Halt Protease Inhibitor Cocktail (100X), followed by adapted volume of Tris buffer pH 7 and 80 µl L-DOPA. Similarly, for inhibited or APO-like activity, 10 µl of sample was mixed with 10 µl of tropolone (140 mM) or trypsin TPCK (14 g l^{-1}), Tris buffer pH 7 and 80 µl L-DOPA. Each measurement was systematically controlled by replacing sample by buffer, always in a final volume reaction of 140 µl. Immediately after L-DOPA addition, PO-like activities were monitored at 25°C for 5 h using Mithras LB 940 luminometer (Berthold, Thoiry, France) at 490 nm [51]. When an inhibited PO-like activity was measured, this value was subtracted from APO and PO-like activities. Tropolone, with its copper chelator and peroxidase substrate properties, ensured that PO-like activity alone was detected (and not peroxidase). Results were also systematically corrected for non-enzymatic

autoxidation of the substrate and were expressed in enzyme unit (1 U) per mg of total protein. One U corresponded to an increase of 0.001 in the absorbance per min at 25°C [57].

2.6. Flow cytometry (FCM) analysis

FCM analyses were performed using a Gallios flow cytometer (Beckman Coulter). In our study, excitation light was provided by a 22 mW blue diode (488 nm), and fluorescence was collected in the FL1 channel with a 525 nm bandpass filter. For each sample, about 20,000 events were acquired. Data were analysed using Kaluza software (Beckman Coulter).

2.6.1. Freshly sampled Hc cytomorphology

Hc morphology was based upon relative flow-cytometric parameters, Forward Scatter (FSC) and Side Scatter (SSC). FSC and SSC commonly measure particle size and internal complexity, respectively. Internal complexity, also reported as granularity, depends upon various inner components of the cells including shape of the nucleus, amount and types of cytoplasmic granules, cytoplasmic inclusions and membrane roughness [59]. Freshly withdrawn Hc was pelleted by 300 × *g* centrifugation for 5 min at 4°C, rinsed in MPS, before to be fixed in 3.7% formaldehyde in MPS and kept in dark at 4°C until FCM analysis.

2.6.2. Phagocytosis assays

Evaluation of phagocytosis was based on the ingestion of carboxylate-modified FluoSpheres® beads (1.0 µm, yellow-green carboxylate-modified FluoSpheres®, Molecular Probes) by Hcs. Phagocytosis was expressed as (*i*) the percentage of cells that had ingested three or more microbeads [60,61], and (*ii*) the average number of microbeads per phagocytic Hcs [18].

Hemolymph-diluted Alsever solution was used to plate Hcs at 1.0×10^6 cells per well in 6-well plates, into which three volumes of sterile artificial seawater (25.5 g l^{-1} NaCl, 6.4 g l^{-1} $MgSO_4$, 5.2 g l^{-1} Hepes, 1.1 g l^{-1} $CaCl_2$, 0.75 g l^{-1} KCl pH 7.4) were added to allow cell adhesion. After 60 min of incubation in dark at 15°C, supernatant was removed and cells were covered with 1 ml modified sterile Leibovitz L-15 medium pH 7.6 (20.2 g l^{-1} NaCl, 0.54 g l^{-1} KCl, 0.6 g l^{-1} $CaCl_2$, 1 g l^{-1} $MgSO_4 \cdot 7H_2O$ and 3.9 g l^{-1} $MgCl_2 \cdot 6H_2O$) [62], supplemented with 2 mM L-glutamine, 100 µg ml^{-1} streptomycin and 60 µg ml^{-1} penicillin G into which FluoSpheres® were added at a ratio of 1:100 (Hc:beads). Hcs from same individual cuttlefish were analyzed at each time.

2.6.2.1. In vitro impact of time and temperature

Hcs were collected from 5 cuttlefish as described in section *2.2*. To determine temperature-dependence of *S. officinalis* phagocytosis, three different temperatures were investigated; one physiological temperature (15°C) and two temperatures (4 and 25°C) out of the thermal window determined by Melzner et al. [23] with 15°C-acclimated cuttlefish. In this context, media with FluoSpheres® were acclimated to different working temperatures before addition to Hcs. Then, 6-well plates were placed in dark at 4, 15 and 25°C CO_2-free incubators, during 30, 60, 120 and 180 min incubation. Afterwards wells were rinsed with MPS to remove bead excess, following by gentle scrapping and centrifugation at 300 × *g* for 5 min at 4°C. Resulting supernatants were removed, pellets resuspended in 3.7% formaldehyde solution in MPS and stored in the dark at 4°C until FCM analysis.

2.6.2.2. In vitro impact of plasma concentrations

To study the plasma opsonization process, FluoSpheres® were added to modified L-15 medium mixed with cell-free plasma at 0 (as control), 1, 10 and 50%. These mixtures were

incubated at 15°C during 1 h before homogenization and addition to cells. After 2 h incubation at 15°C, cells were treated as previously described (cf *2.6.2.1.*) for FCM analysis.

In parallel, bead phagocytosis was performed in modified L-15 medium or 100% plasma, and Hcs analysed by TEM as described in section *2.4.2*.

2.7. Data analysis

Residual distributions were tested for normality (Shapiro test) as well as homogeneity of variances (Levene test). Student's *t*-test was used to compare Hc concentrations between male and female individuals, specific activities between Hc and plasma compartments, PO- and APO-like activities in each compartment, and phagocytic parameters between control and several plasma treatments. One-way analysis of variance (ANOVA) followed by non-parametric pairwise permutational *t*-tests ($N<30$) was used to determine the impact of temperature on phagocytic parameters at each time. Analysis of covariance (ANCOVA) was used to compare phagocytic parameter time-evolution as function of the temperature. All results are expressed and displayed as mean ± standard deviation (SD). The statistical significance was designed as being at the level of $p<0.05$. R software was used for statistics and graphics.

3. Results and Discussion

Little is known about cephalopod Hcs, while Hc populations have been extensively studied in other mollusks (bivalves and gastropods). Our study provides the most comprehensive description of the circulating Hc population in the cuttlefish *S. officinalis* by using FCM, light and electron microscopy. We also report biochemical- and phagocytosis analysis of Hc interaction with plasma.

3.1. Hc viability and concentration

Hc viability in all cuttlefish used in this study was higher than 99% (data not shown), and no Hc concentration difference was observed between males ($7.20 \pm 5.70 \times 10^6$ cells ml^{-1}; N=18) and females ($7.27 \pm 5.75 \times 10^6$ cells ml^{-1}; N=13). Consequently, we obtained a mean Hc concentration in hemolymph of *S. officinalis* of $7.23 \pm 5.62 \times 10^6$ cells ml^{-1} ranging from 0.92 to 20.31×10^6 cells ml^{-1}. This mean concentration and concentration variability are consistent with reports on cephalopod Hcs (Table 1). Although highly variable, the Hc concentration of *S. officinalis* appeared slightly higher than that of the loliginidae *Sepioteuthis lessoniana*, similar to that of the sepiolidae *Euprymna scolopes*, and lower than that of Octopodidae, where the highest Hc concentrations within cephalopods are found (10×10^6 cells ml^{-1}) [40,42,63–67]. Generally, Hcs of gastropod and bivalve mollusks appear less concentrated with most values ranging between 1 and 5×10^6 cells ml^{-1} (Table 1) [6,7,9,11,12,18–20,59,68–75], albeit with population-dependent variation [7,12,76].

3.2. Hc identification and characterization

3.2.1. Light microscopy

After adhesion, fresh cuttlefish Hcs rapidly displayed many thin pseudopodia, and most cells contained refringent and non-refringent granules of various densities in their

298 cytoplasm (Fig. 1). Among different stains used, Wright's differential staining allowed the
299 best observation of spontaneously adhering Hcs. A single cell type with large, lobate nucleus,
300 slightly basophilic cytoplasm and acidophilic granules was identified (Fig. 2A). Lucent
301 vesicles were also observed in the cytoplasm of some cells. NR uptake revealed dense
302 lysosomal system in most cells (Fig. 2B). According to the classification of bivalve Hcs, 2
303 main classes are usually accepted: granulocytes with cytoplasmic granules and hyalinocytes
304 with few or no granules [77]. Based on the high granule density found in most Hcs, we
305 classify *S. officinalis* Hcs as granulocytes. These observations are consistent with the majority
306 of studies performed in Octopodidae [31,34,41,78,79], Sepiidae [33] and Sepiolidae [42,80],
307 which reported one granular cell population circulating in the hemolymph and also called
308 macrophage-like Hc [34,81].
309
310 *3.2.2. Electron microscopy*
311 SEM observations of circulating cuttlefish Hcs showed a single cell type of 10.3 ± 0.8
312 µm in diameter and able to form numerous pseudopodia (Fig. 3A-B), consistent with the
313 above described light microscopy observations. This cell size is consistent with the 8-10 µm
314 cell diameter measured on non-circulating mature Hcs in the cuttlefish white bodies
315 (leukopoietic tissues) [33] and appeared slightly lower than octopod *O. vulgaris* and *E.*
316 *cirrhosa* Hcs: 11.6 ± 1.2 and 12-15 µm, respectively [63,82].
317 TEM observations of circulating Hcs highlighted a large lobate nucleus without nucleoli
318 but highly condensed chromatin mainly localized along the inner surface of the nuclear
319 membrane (Fig. 3C). The cytoplasm of most cells contained various sizes and densities of two
320 distinct inclusion types (Fig. 3D): electron-dense granules corresponding to lysosomes [33],
321 and electron-lucent membrane-surrounded vesicles, containing various densities of molecules
322 with similar size and circular shape as Hcy molecules (Fig. 3E-F; [83–87]). These molecules

are referred to as Hcy-like hereafter. In contrast to *E. cirrhosa* and *O. vulgaris* Hcs, neither different electron-dense granules nor lipid droplets were observed [31,34,63], suggesting different granule contents between these cephalopods. Mitochondria, Golgi apparatus and rough endoplasmic reticulum that often surrounded the nucleus were also observed in these cells (Fig. 3C inset).

3.3. Enzymatic assays

Hydrolytic enzyme lysozymes and acid phosphatases were detected in Hc extract alone (Table 2), consistent with their known lysosomal distribution [88,89]. These data are in agreement with carbohydrates and acid phosphatases detected by stainings in *E. cirrhosa* Hcs [66] and suggest their synthesis in *S. officinalis* Hcs or earlier during their maturation [66,90]. PI activities were exclusively found in plasma (Table 2), corresponding at least in part to the already described α_2-macroglobulin activity – the second most abundant protein in *S. officinalis* plasma [91–93]. Interestingly, PIs were recently reported in *E. cirrhosa* and *E. scolopes* Hcs [31,42], underlying the need for future investigations.

PO-like activities were measured in both hemolymph compartments (Table 2). Siddiqui et al. [94] showed in *S. officinalis* that plasma-associated PO-activity resulted from Hcy, which molecule shares a structurally and functionally equivalent active site with POs [95]. Therefore, PO-like activities found in Hc extracts probably result, at least in part, from Hcy presence in electron-lucent vesicles (TEM analysis). We note that PO activity was not previously detected in cephalopod Hcs. In contrast, proPO activation – the difference between PO- and APO-like activity, occurred in Hc extract alone (p=0.01).

3.4. FCM analysis

3.4.1. Fresh Hc cytogram

According to the criteria of cell size (FSC) and cell complexity (SSC), FCM supported the presence of a single Hc population in cuttlefish (Fig. 4A), albeit with variable internal complexity in some individuals (Fig. 4B), consistent with the above described TEM observations. Notably, recent *O. vulgaris* Hc characterization using TEM and FCM reported 2 circulating granulocyte morphs based on size, which were interpreted as different maturating stages of the same cell type [63]. Consistently, a study of *S. officinalis* Hc synthesis suggested a Hc maturation model with a single cell precursor [33]. This cephalopod organization is distinct from that of bivalves and gastropods, where most Hc studies reported several circulating Hc types derived from one or more cell precursors (e.g. [5,8,9,11,15,17,18,20,32,96,97]). Our results further support the presence of a single mature circulating cell type in the Hc population of cephalopods.

3.4.2. Phagocytosis experiments

3.4.2.1. Time and temperature

Both phagocytosis parameters (i.e. percentage of phagocytic Hcs and quantity of ingested beads) appeared time-dependent at all temperatures tested (Fig. 5).

After 30 min, 35.5, 40.1, and 41.7% of cells were phagocytic at 4, 15 and 25°C, respectively, subsequently reaching 63.3, 70.6 and 69.8% after 180 min (Fig. 5A). These phagocytic percentages are consistent with previous observations of Hcs in *O. vulgaris* and *E. cirrhosa* where 50 and 70% of phagocytic cells were reported, respectively [40,98]. In contrast, a lower phagocytic percentage (≤ 13%) was recently reported for *O. vulgaris* Hcs after 120 min incubation at 15°C [63]. The filtered seawater used as media during this *in vitro* experiment may account for this lower rate. Overall, our results are among the highest phagocytic percentages reported among mollusks, regardless of experimental conditions (e.g. [5–7,11,12,15,18,72,75,96,99–104].

373 The time-dependent evolution of phagocytosis measured in our study is consistent with
374 previous findings on Hcs of mollusk bivalves [5,12,99,102,105] and gastropods [15,18,106],
375 but also crustacean [107] and fish blood cells [108]. Within cephalopods, Malham et al. [98]
376 showed similar evolution on *E. cirrhosa* Hcs, whereas Rodriguez-Dominguez et al. [40]
377 reported constant *O. vulgaris* Hc phagocytic percentages from 45 to 120 min incubation at
378 22°C.

379 Notably, temperature sensitivity appears species-specific in cephalopods, as no effects
380 were observed in our study, whereas negative effects of low temperatures (4-10°C) were
381 reported on Hc phagocytosis rate in *O. vulgaris* [40], and *E. cirrhosa* [98]. Although
382 temperatures used were extremes and out of the thermal window of 15°C-acclimated
383 cuttlefish [23] (25°C - inducing anaerobic metabolism, and 4°C - a lethal temperature [109]),
384 no significant effects on phagocytosis parameters were found in our study. This low effect of
385 temperature on Hc phagocytosis ability is consistent with the eurythermy of *S. officinalis*.

386 The quantity of ingested beads measured by FCM evolved in similar ways as the
387 percentage of phagocytic Hcs. Mean quantity of beads in Hcs increased during the entire
388 experiment from 5.9, 7.0 and 6.8 beads $cell^{-1}$ after 30 min to 16.4, 18.7 and 16.9 beads $cell^{-1}$
389 after 180 min at 4, 15 and 25°C, respectively (Fig. 5B). Concurrent TEM observations
390 confirmed the number of ingested beads registered by FCM (Fig. 6A) and visually
391 demonstrated the engulfment process with (1) Hc-bead adhesion, (2) bead internalization by
392 almost continuous close contact between membrane and particle, and (3) closing phagosome
393 (Fig. 6B-C). Occasionally, we also observed lysosomal fusion with phagosome (Fig. 6D).

394 Our phagocytosis assay revealed similar rates of bead engulfment as those found in *O.*
395 *vulgaris* [40], but higher rates than in the mollusk bivalve *Perna viridis* and gastropods
396 *Lymnaea stagnalis*, *Haliotis discus discus* and *Turbo cornutus* [12,18,106], highlighting
397 higher engulfment capacity of cephalopod Hcs. Nevertheless, such differences could be

398 explained by the high number of beads per cell used in our study (1:100) compared to those of
399 previous ones (≤ 1:10).
400
401 *3.4.2.2. Opsonization assay*
402 As observed under FCM, opsonization experiments differently affected Hc phagocytosis
403 percentage and engulfed bead number. While phagocytosis occurred without incubation of
404 Hcs or beads in plasma, an increase in ingested bead number occurred after incubation in 1 or
405 10% plasma (p=0.008 and 0.045, respectively) (Fig. 7). In contrast, incubation of beads and
406 Hcs in 50% plasma led to a decrease of phagocytosis percentage (p=0.04). TEM observations
407 of phagocytosis conducted with plasma revealed a bead-coating by Hcy-like molecules (Fig.
408 8A-B) as previously suggested in cephalopods [82,98,110]. This observation could explain
409 Hcy presence in Hc electron-lucent vesicles. Moreover, Hcy-like molecule presence in
410 bridges between beads (Fig. 8C) suggested an agglutinating function, consistent with the
411 increasing engulfed bead number observed at 1 and 10% plasma (Fig. 7). Such findings are
412 consistent with a recent *Octopus maya* plasma agglutinin (OmA) characterization, showing
413 homology between OmA subunits and one functional unit of Hcy from *Octopus dolfeini* [111].
414 Moreover, bead engulfment increased after as low as 1% plasma addition, underlying the high
415 concentration of the molecule in charge of this process, and Hcy is known to represent more
416 than 90% of cephalopod plasma proteins [98,112–114]. Such agglutinating function could
417 also explain the phagocytic percentage decrease occurring with 50% plasma. Indeed,
418 important bead agglutination might limit the availability of these particles for phagocytic
419 process by increasing the size of particles to engulf. Ballarin et al. [115] described a similar
420 phagocytic decrease resulting from agglutinins in the ascidian *Botryllus schlosseri* after yeast
421 pre-incubation in high plasma concentrations (≥ 50%). In cephalopods, this Hcy property
422 could explain the decrease of phagocytosis by *O. vulgaris* Hcs measured after pre-incubation

of zymosan in 100% plasma [40], because of zymosan particle (about 3 µm) aggregation. Malham et al. [98] and Ballarin et al. [115] highlighted also the importance of phagocytose duration in this type of study, as phagocytosis enhancement after plasma incubation mainly occurred after 30 min. This is consistent with our study and that of Rodriguez-Dominguez et al. [40] which report plasma-dependent phagocytosis decrease after 120 and 90 min of phagocytosis duration, respectively. Our results demonstrate the presence of a Hcy-like coating molecule with agglutinin function in *S. officinalis* plasma, which can modulate phagocytosis according to (1) pre-incubation plasma concentration and (2) phagocytosis duration.

4. Conclusions

Our study demonstrates, using FCM, light- and electron-microscopy, that a single granulocyte population with variable internal complexity circulates in the hemolymph of *S. officinalis*, as in other cephalopods. Acid phosphatase, lysozyme, and for the first time in cephalopods proPO system enzymes were detected in Hcs, but not in plasma [31,116]. These cells were able to recognize and incorporate foreign material at high rate independently of temperature and without need for plasma. Concurrent TEM and FCM analysis suggested a role for Hcy in foreign particle coating probably associated with its hypothesized agglutinin function. These data provide important information to understand the Hc-mediated immunity in the common cuttlefish, and a useful background for future studies of cephalopod Hcs.

Acknowledgments

This work was supported by the European, Interreg IV-A CHRONEXPO project. This study was partly conducted in the CREC (Centre de Recherche en Environnement Côtier) at Luc-sur-mer (Normandie, France). The authors thank Beatrice Adeline for technical support in cytological analysis and Dr Pierre Le Pabic for advices and help in English.

References

[1] Loker ES, Adema CM, Zhang S-M, Kepler TB. Invertebrate immune systems-not homogeneous, not simple, not well understood. Immunol Rev 2004;198:10–24.

[2] Rowley AF, Powell A. Invertebrate immune systems specific, quasi-specific, or nonspecific? J Immunol 2007;179:7209–14.

[3] Ponder WF, Lindberg DR. Molluscan evolution and phylogeny: an introduction. In: Ponder WF, Lindberg DR, editors. Phylogeny Evol. Mollusca, Berkeley and Los Angeles, California: University of California Press; 2008, p. 1–18.

[4] Aladaileh S, Rodney P, Nair S V., Raftos DA. Characterization of phenoloxidase activity in Sydney rock oysters (*Saccostrea glomerata*). Comp Biochem Physiol Part B, Biochem & Mol Biol 2007;148:470–80.

[5] Hong H-K, Kang H-S, Le TC, Choi K-S. Comparative study on the hemocytes of subtropical oysters *Saccostrea kegaki* (Torigoe & Inaba, 1981), *Ostrea circumpicta* (Pilsbry, 1904), and *Hyotissa hyotis* (Linnaeus, 1758) in Jeju Island, Korea: Morphology and functional aspec. Fish & Shellfish Immunol 2013;35:2020–5.

[6] Wootton EC, Pipe RK. Structural and functional characterisation of the blood cells of the bivalve mollusc, *Scrobicularia plana*. Fish & Shellfish Immunol 2003;15:249–62.

[7] Wang Y, Hu M, Chiang MWL, Shin PKS, Cheung SG. Characterization of subpopulations and immune-related parameters of hemocytes in the green-lipped mussel *Perna viridis*. Fish & Shellfish Immunol 2012;32:381–90.

[8] Salimi L, Jamili S, Motalebi A, Eghtesadi-Araghi P, Rabbani M, Rostami-Beshman M. Morphological characterization and size of hemocytes in *Anodonta cygnea*. J Invertebr Pathol 2009;101:81–5.

[9] Matozzo V, Rova G, Marin MG. Haemocytes of the cockle *Cerastoderma glaucum*: morphological characterisation and involvement in immune responses. Fish & Shellfish Immunol 2007;23:732–46.

[10] López C, Carballal MJ, Azevedo C, Villalba A. Morphological characterization of the hemocytes of the clam, *Ruditapes decussatus* (Mollusca: Bivalvia). J Invertebr Pathol 1997;69:51–7.

[11] Donaghy L, Kim B-K, Hong H-K, Park H-S, Choi K-S. Flow cytometry studies on the populations and immune parameters of the hemocytes of the Suminoe oyster, *Crassostrea ariakensis*. Fish & Shellfish Immunol 2009;27:296–301.

[12] Donaghy L, Volety AK. Functional and metabolic characterization of hemocytes of the green mussel, *Perna viridis*: *in vitro* impacts of temperature. Fish & Shellfish Immunol 2011;31:808–14.

[13] Allam B, Ashton-Alcox K a., Ford SE. Flow cytometric comparison of haemocytes from three species of bivalve molluscs. Fish & Shellfish Immunol 2002;13:141–58.

[14] Chang S, Tseng S, Chou H. Morphological characterization via light and electron microscopy of two cultured bivalves: A comparison study between the Hard clam (*Meretrix lusoria*) and Pacific Oyster (*Crassostrea gigas*). Zool Stud 2005;44:144–52.

[15] Travers M-A, Mirella da Silva P, Le Goïc N, Marie D, Donval A, Huchette S, et al. Morphologic, cytometric and functional characterisation of abalone (*Haliotis tuberculata*) haemocytes. Fish & Shellfish Immunol 2008;24:400–11.

[16] Matricon-Gondran M, Letocart M. Internal defenses of the snail *Biomphalaria glabrata*. J Invertebr Pathol 1999;74:248–54.

[17] Mahilini HM, Rajendran A. Categorization of hemocytes of three gastropod species *Trachea vittata* (Muller), *Pila globosa* (Swainson) and *Indoplanorbis exustus* (Dehays). J Invertebr Pathol 2008;97:20–6.

[18] Donaghy L, Hong H-K, Lambert C, Park H-S, Shim WJ, Choi K-S. First characterisation of the populations and immune-related activities of hemocytes from two edible gastropod species, the disk abalone, *Haliotis discus discus* and the spiny top shell, *Turbo cornutus*. Fish & Shellfish Immunol 2010;28:87–97.

[19] Barracco MA, Steil AA, Gargioni R. Morphological characterization of the hemocytes of the pulmonate snail *Biomphalaria tenagophila*. Mem Inst Oswaldo Cruz 1993;88:73–83.

[20] Accorsi A, Bucci L, de Eguileor M, Ottaviani E, Malagoli D. Comparative analysis of circulating hemocytes of the freshwater snail *Pomacea canaliculata*. Fish & Shellfish Immunol 2013;34:1260–8.

[21] Ford LA. Host defense mechanisms of cephalopods. Annu Rev Fish Dis 1992;2:25–41.

[22] Castellanos-Martínez S, Gestal C. Pathogens and immune response of cephalopods. J Exp Mar Bio Ecol 2013;447:14–22.

[23] Melzner F, Mark FC, Pörtner H-O. Role of blood-oxygen transport in thermal tolerance of the cuttlefish, *Sepia officinalis*. Integr Comp Biol 2007;47:645–55.

[24] Pierce GJ, Stowasser G, Hastie LC, Bustamante P. Geographic, seasonal and ontogenetic variation in cadmium and mercury concentrations in squid (Cephalopoda: Teuthoidea) from UK waters. Ecotoxicol Environ Saf 2008;70:422–32.

[25] Sykes A V, Domingues PM, Correia M, Andrade JP. Cuttlefish culture - State of the art and future trends. Life & Environ 2006;56:129–37.

[26] Berger E. Aquaculture of *Octopus* species : present status, problems andperspectives. Plymouth Student Sci 2010;4:384–99.

519 [27] Uriarte I, Iglesias J, Domingues P, Rosas C, Viana MT, Navarro JC, et al. Current
520 Status and Bottle Neck of Octopod Aquaculture: The Case of American Species. J
521 World Aquac Soc 2011;42:735–52.

522 [28] Reid A, Jereb P, Roper CFE. Cephalopods of the world. An annotated and illustrated
523 catalogue of species known to date. Volume 1. Chambered nautiluses and sepioids
524 (Nautilidae, Sepiidae, Sepiolidae, Sepiadariidae, Idiosepiidae and Spirulidae). In: Jereb
525 P, Roper CFE, editors. FAO Species Cat. Fish. Purp. No. 4, Vol. 1, Rome: 2005, p. 57–
526 152.

527 [29] Payne AG, Agnew DJ, Pierce GJ. Trends and assessment of cephalopod fisheries. Fish
528 Res 2006;78:1–3.

529 [30] Soudant P, E Chu F-L, Volety A. Host-parasite interactions: Marine bivalve molluscs
530 and protozoan parasites, *Perkinsus* species. J Invertebr Pathol 2013;114:196–216.

531 [31] Malham SK. Immunobiology of *Eledone cirrhosa* (Lamarck). University of Wales,
532 Bangor, North Wales, UK, 1996.

533 [32] Wang L, Qiu L, Zhou Z, Song L. Research progress on the mollusc immunity in China.
534 Dev & Comp Immunol 2013;39:2–10.

535 [33] Claes MF. Functional morphology of the white bodies of the cephalopod mollusc *Sepia*
536 *officinalis*. Acta Zool 1996;77:173–90.

537 [34] Cowden RR, Curtis SK. Cephalopods. In: Ratcliff NA, Rowley AF, editors. Invertebr.
538 Blood Cells. Gen. Asp. Anim. without True Circ. Syst. to Cephalopods, London:
539 Academic press; 1981, p. 301–23.

540 [35] Donaghy L, Lambert C, Choi K-S, Soudant P. Hemocytes of the carpet shell clam
541 (*Ruditapes decussatus*) and the Manila clam (*Ruditapes philippinarum*): Current
542 knowledge and future prospects. Aquaculture 2009;297:10–24.

543 [36] Beninger PG, Le Pennec G, Le Pennec M. Demonstration of nutrient pathway from the
544 digestive system to oocytes in the gonad intestinal loop of the scallop *Pecten maximus*
545 L. Biol Bull 2003;205:83–92.

546 [37] Matozzo V, Ballarin L, Pampanin DM, Marin MG. Effects of copper and cadmium
547 exposure on functional responses of hemocytes in the clam, *Tapes philippinarum*. Arch
548 Environ Contam Toxicol 2001;41:163–70.

549 [38] Montes JF, Durfort M, García-Valero J. Cellular defence mechanism of the clam *Tapes*
550 *semidecussatus* against infection by the protozoan *Perkinsus* sp . Cell Tissue Res
551 1995;279:529–38.

552 [39] Mount AS, Wheeler AP, Paradkar RP, Snider D. Hemocyte-mediated shell
553 mineralization in the eastern oyster. Science 2004;304:297–300.

554 [40] Rodríguez-Domínguez H, Soto-Búa M, Iglesias-Blanco R, Crespo-González C, Arias-
555 Fernández C, García-Estévez J. Preliminary study on the phagocytic ability of *Octopus*

556 *vulgaris* Cuvier, 1797 (Mollusca: Cephalopoda) haemocytes in vitro. Aquaculture
557 2006;254:563–70.

558 [41] Bolognari A. Morfologia, struttura e funzione del “corpo bianco” dei cefalopodi. II.
559 Struttura e funzione. Arch Zool Ital 1951;36:252–87.

560 [42] Collins AJ, Schleicher TR, Rader BA, Nyholm S V. Understanding the role of host
561 hemocytes in a squid/*Vibrio* symbiosis using transcriptomics and proteomics. Front
562 Immunol 2012;3:91.

563 [43] Boucaud-Camou E, Boismery J. The migrations of the cuttlefish (*Sepia officinalis* L.)
564 in the English Channel. The Cuttlefish, Caen: Centre de publication de l’Université de
565 Caen; 1991, p. 179–89.

566 [44] Wang J, Pierce GJ, Boyle PR, Denis V, Robin J, Bellido JM. Spatial and temporal
567 patterns of cuttlefish (*Sepia officinalis*) abundance and environmental influences – a
568 case study using trawl fishery data in French Atlantic coastal , English Channel , and
569 adjacent waters. ICES J Mar Sci 2003;3139:1149–58.

570 [45] Andrews PLR, Darmaillacq A-S, Dennison N, Gleadall IG, Hawkins P, Messenger JB,
571 et al. The identification and management of pain, suffering and distress in cephalopods,
572 including anaesthesia, analgesia and humane killing. J Exp Mar Bio Ecol 2013;447:46–
573 64.

574 [46] King AJ, Henderson SM, Schmidt MH, Cole AG, Adamo SA. Using ultrasound to
575 understand vascular and mantle contributions to venous return in the cephalopod *Sepia*
576 *officinalis* L. J Exp Biol 2005;208:2071–82.

577 [47] Bachère E, Chagot D, Grizel H. Separation of *Crassostrea gigas* hemocytes by density
578 gradient centrifugation and counterflow centrifugal elutriation. Dev & Comp Immunol
579 1988;12:549–59.

580 [48] Oestmann DJ, Scimeca JM, Forsythe J, Hanlon RT, Lee P. Special considerations for
581 keeping cephalopods in laboratory facilities. J Am Assoc Lab Anim Sci 1997;36:89–
582 93.

583 [49] Lowe DM, Soverchiab C, Moore MN. Lysosomal membrane responses in the blood
584 and digestive cells of mussels experimentally exposed to fluoranthene. Aquat Toxicol
585 1995;33:105–12.

586 [50] Venable JH, Coggeshall R. A simplified lead citrate stain for use in electron
587 microscopy. J Cell Biol 1965;25:407–8.

588 [51] Luna-Acosta A. Les phénoloxydases chez l’huître creuse *Crassostrea gigas* :
589 biomarqueurs potentiels de stress environnemental. Université de La Rochelle, 2010.

590 [52] Safi G. Etude de la variabilité spatio-temporelle des caractéristiques physiologiques des
591 jeunes stades de vie de la seiche *Sepia officinalis* L . en Manche. Université de Caen
592 Basse-Normandie, 2013.

[53] Bradford MM. A rapid and sensitive method for the quantitation of microgram quantities of protein utilizing the principle of protein-dye binding. Anal Biochem 1976;72:248–54.

[54] Moyano FJ, Díaz M, Alarcón FJ, Sarasquete MC. Characterization of digestive enzyme activity during larval development of gilthead seabream (*Sparus aurata*). Fish Physiol Biochem 1996;15:121–30.

[55] Malham SK, Runham NW, Secombes CJ. Lysozyme and antiprotease activity in the lesser octopus *Eledone cirrhosa* (Lam.) (Cephalopoda). Dev & Comp Immunol 1998;22:27–37.

[56] Thompson I, Choubert G, Houlihan DF, Secombes CJ. The effect of dietary vitamin A and astaxanthin on the immunocompetence of rainbow trout. Aquaculture 1995;133:91–102.

[57] Le Pabic C, Safi G, Serpentini A, Lebel J-M, Robin J-P, Koueta N. Prophenoloxidase system, lysozyme and protease inhibitor distribution in the common cuttlefish *Sepia officinalis*. Comp Biochem Physiol Part B, Biochem & Mol Biol 2014;172-173B:96–104.

[58] Lacoue-Labarthe T, Bustamante P, Hörlin E, Luna-Acosta A, Bado-Nilles A, Thomas-Guyon H. Phenoloxidase activation in the embryo of the common cuttlefish *Sepia officinalis* and responses to the Ag and Cu exposure. Fish & Shellfish Immunol 2009;27:516–21.

[59] Donaghy L, Jauzein C, Volety AK. First report of severe hemocytopenia and immunodepression in the sunray venus clam, *Macrocallista nimbosa*, a potential new aquaculture species in Florida. Aquaculture 2012;364-365:247–51.

[60] Hégaret H, Wikfors GH, Soudant P. Flow cytometric analysis of haemocytes from eastern oysters, *Crassostrea virginica*, subjected to a sudden temperature elevation. J Exp Mar Bio Ecol 2003;293:249–65.

[61] Auffret M, Rousseau S, Boutet I, Tanguy A, Baron J, Moraga D, et al. A multiparametric approach for monitoring immunotoxic responses in mussels from contaminated sites in Western Mediterranea. Ecotoxicol Environ Saf 2006;63:393–405.

[62] Domart-coulon I, Doumenc D, Auzoux-bordenave S. Identification of media supplements that improve the viability of primarily cell cultures of *Crassostrea gigas* oysters. Cytotechnology 1994;16:109–20.

[63] Castellanos-Martínez S, Prado-Alvarez M, Lobo-da-Cunha A, Azevedo C, Gestal C. Morphologic, cytometric and functional characterization of the common octopus (*Octopus vulgaris*) hemocytes. Dev & Comp Immunol 2014;44:50–8.

[64] Heming TA, Vanoye CG, Brown SE, Bidani A. Cytoplasmic pH recovery in acid-loaded haemocytes of squid (*Sepioteuthis lessoniana*). J Exp Biol 1990;148:385–94.

630 [65] Collins AJ, Nyholm S V. Obtaining hemocytes from the Hawaiian bobtail squid
631 *Euprymna scolopes* and observing their adherence to symbiotic and non-symbiotic
632 bacteria. J Vis Exp 2010:3–5.

633 [66] Malham SK, Coulson CL, Runham NW. Effects of repeated sampling on the
634 haemocytes and haemolymph of *Eledone cirrhosa* (Lam.). Comp Biochem Physiol Part
635 A Mol & Integr Physiol 1998;121:431–40.

636 [67] Malham SK, Lacoste A, Gélébart F, Cueff A, Poulet SA. A first insight into stress-
637 induced neuroendocrine and immune changes in the octopus *Eledone cirrhosa*. Aquat
638 Living Resour 2002;15:187–92.

639 [68] Wootton EC, Dyrynda EA, Ratcliffe NA. Bivalve immunity: comparisons between the
640 marine mussel (*Mytilus edulis*), the edible cockle (*Cerastoderma edule*) and the razor-
641 shell (*Ensis siliqua*). Fish & Shellfish Immunol 2003;15:195–210.

642 [69] Barracco MA, Medeiros ID, Moreira FM. Some haemato-immunological parameters in
643 the mussel *Perna perna*. Fish & Shellfish Immunol 1999;9:387–404.

644 [70] Goedken M, De Guise S. Flow cytometry as a tool to quantify oyster defence
645 mechanisms. Fish & Shellfish Immunol 2004;16:539–52.

646 [71] Zhang W, Wu X, Wang M. Morphological, structural, and functional characterization
647 of the haemocytes of the scallop, *Argopecten irradians*. Aquaculture 2006;251:19–32.

648 [72] Nakayama K, Nomoto A, Nishijima M, Maruyama T. Morphological and functional
649 characterization of hemocytes in the giant clam *Tridacna crocea*. J Invertebr Pathol
650 1997;69:105–11.

651 [73] Xie Y, Hu B, Wen C, Mu S. Morphology and phagocytic ability of hemocytes from
652 *Cristaria plicata*. Aquaculture 2011;310:245–51.

653 [74] Pampanin DM, Marin MG, Ballarin L. Morphological and cytoenzymatic
654 characterization of haemocytes of the venus clam *Chamelea gallina*. Dis Aquat Organ
655 2002;49:227–34.

656 [75] Jauzein C, Donaghy L, Volety AK. Flow cytometric characterization of hemocytes of
657 the sunray venus clam *Macrocallista nimbosa* and influence of salinity variation. Fish
658 & Shellfish Immunol 2013;35:716–24.

659 [76] Santarém MM, Robledo JAF, Figueras A. Seasonal changes in hemocytes and serum
660 defense factors in the blue mussel *Mytilus galloprovincialis*. Dis Aquat Organ
661 1994;18:217–22.

662 [77] Cheng TC. Bivalves. In: N.A.R.A.R., editor. Invertebr. blood cells, London: Academic
663 press; 1981, p. 233–300.

664 [78] Cowden RR, Curtis SK. Observations on living cells dissociated from the leukopoietic
665 organ of *Octopus briareus*. Exp Mol Pathol 1973;19:178–85.

[79] Kondo M, Tomanaga S, Takahashi Y. Morphology of octopus hemocytes. J Natl Fish Univ 2003;4:157–64.

[80] Heath-Heckman EAC, McFall-Ngai MJ. The occurrence of chitin in the hemocytes of invertebrates. Zoology 2011;114:191–8.

[81] Nyholm S V, McFall-Ngai MJ. Sampling the light-organ microenvironment of *Euprymna scolopes*: description of a population of host cells in association with the bacterial symbiont *Vibrio fischeri*. Biol Bull 1998;195:89–97.

[82] Stuart AE. The reticulo-endothelial apparatus of the lesser octopus, *Eledone cirrhosa*. J Pathol Bacteriol 1968;96:401–12.

[83] Bergmann S, Lieb B, Ruth P, Markl J. The hemocyanin from a living fossil, the cephalopod *Nautilus pompilius*: protein structure, gene organization, and evolution. J Mol Evol 2006;62:362–74.

[84] Dilly PN, Messenger JB. The branchial gland: a site of haemocyanin synthesis in *Octopus*. Z Zellforsch Mikrosk Anat 1972;132:193–201.

[85] Muzii E. Intracellular polymerized haemocyanin in the branchial gland of a cephalopod. Cell Tissue Res 1981;220:435–8.

[86] Boisset N, Mouche F. *Sepia officinalis* hemocyanin: A refined 3D structure from field emission gun cryoelectron microscopy. J Mol Biol 2000;296:459–72.

[87] Martoja M, Marcaillou C. Localisation cytologique du cuivre et de quelques autres métaux dans la glande digestive de la seiche, *Sepia officinalis* L. (Mollusque Céphalopode). Can J Fish Aquat Sci 1993;50:542–50.

[88] Blasco J, Puppo J, Sarasqnete MC. Acid and alkaline phosphatase activites in the clam *Ruditapes philippinarum*. Mar Biol 1993;115:113–8.

[89] Fiołka MJ, Zagaja MP, Hułas-Stasiak M, Wielbo J. Activity and immunodetection of lysozyme in earthworm *Dendrobaena veneta* (Annelida). J Invertebr Pathol 2012;109:83–90.

[90] Cowden RR. Some cytological and cytochemical observations on the leucopoietic organs, the “White Bodies”, of *Octopus vulgaris*. J Invertebr Pathol 1972;19:113–9.

[91] Thøgersen IB, Salvesen G, Brucato FH, Pizzo S V, Enghild JJ. Purification and characterization of an α-macroglobulin proteinase inhibitor from the mollusc *Octopus vulgaris*. Biochem J 1992;285:521–7.

[92] Armstrong PB. Humoral immunity: α_2-macroglobulin activity in the plasma of mollusks. The Veliger 1992;35:161–4.

[93] Vanhoorelbeke K, Goossens A, Gielsens C, Préaux G. An α_2-macroglobulin-like proteinase inhibitor in the haemolymph of the Decabrachia cephalopod *Sepia officinalis*. Arch Int Physiol Biochim Biophys 1994;102:B25.

[94] Siddiqui NI, Akosung RF, Gielens C. Location of intrinsic and inducible phenoloxidase activity in molluscan hemocyanin. Biochem Biophys Res Commun 2006;348:1138–44.

[95] Campello S, Beltramini M, Giordano G, Di Muro P, Marino SM, Bubacco L. Role of the tertiary structure in the diphenol oxidase activity of *Octopus vulgaris* hemocyanin. Arch Biochem Biophys 2008;471:159–67.

[96] Prado-Alvarez M, Romero A, Balseiro P, Dios S, Novoa B, Figueras A. Morphological characterization and functional immune response of the carpet shell clam (*Ruditapes decussatus*) haemocytes after bacterial stimulation. Fish & Shellfish Immunol 2012;32:69–78.

[97] Rebelo MDF, Figueiredo EDS, Mariante RM, Nóbrega A, de Barros CM, Allodi S. New insights from the oyster *Crassostrea rhizophorae* on bivalve circulating hemocytes. PLoS One 2013;8:e57384.

[98] Malham SK, Runham NW, Secombes CJ. Phagocytosis by haemocytes from the Lesser Octopus *Eledone cirrhosa*. Iberus 1997;15:1–11.

[99] Ordas MC, Novoa B, Figueras A. Phagocytosis inhibition of clam and mussel haemocytes by *Perkinsus atlanticus* secretion products . Fish & Shellfish Immunol 1999;9:491–503.

[100] Carballal MJ, López C, Azevedo C, Villalba A. *In vitro* study of phagocytic ability of *Mytilus galloprovincialis* Lmk. haemocytes. Fish & Shellfish Immunol 1997;7:403–16.

[101] Di G, Zhang Z, Ke C. Phagocytosis and respiratory burst activity of haemocytes from the ivory snail, *Babylonia areolata*. Fish & Shellfish Immunol 2013;35:366–74.

[102] Cima F, Matozzo V, Marin MG, Ballarin L. Haemocytes of the clam *Tapes philippinarum* (Adams & Reeve, 1850): morphofunctional characterisation. Fish & Shellfish Immunol 2000;10:677–93.

[103] Xue QG, Renault T, Chilmonczyk S. Flow cytometric assessment of haemocyte sub-populations in the European flat oyster, *Ostrea edulis*, haemolymph. Fish & Shellfish Immunol 2001;11:557–67.

[104] Gorbushin AM, Iakovleva N V. Functional characterization of *Littorina littorea* (Gastropoda: Prosobranchia) blood cells. J Mar Biol Assoc UK 2007;87:741.

[105] Canesi L, Gallo G, Gavioli M, Pruzzo C. Bacteria-hemocyte interactions and phagocytosis in marine bivalves. Microsc Res Tech 2002;57:469–76.

[106] Adema CM, van Deutekom-Mulder EC, van der Knaap WPW, Meuleman A, Sminia T. Generation of oxygen radicals in hemocytes of the snail *Lymnaea stagnalis* in relation to the rate of phagocytosis. Dev Comp Immunol 1991;15:17–26.

[107] Raman T, Arumugam M, Mullainadhan P. Agglutinin-mediated phagocytosis-associated generation of superoxide anion and nitric oxide by the hemocytes of the

739 giant freshwater prawn *Macrobrachium rosenbergii*. Fish & Shellfish Immunol
740 2008;24:337–45.

741 [108] Harford AJ, O'Halloran K, Wright PF a. Flow cytometric analysis and optimisation for
742 measuring phagocytosis in three Australian freshwater fish. Fish & Shellfish Immunol
743 2006;20:562–73.

744 [109] Richard A. Contribution à l'étude expérimentale de la croissance et de la maturation
745 sexuelle de *Sepia officinalis* L. (Mollusque Céphalopode). Université de Lille, 1971.

746 [110] Beuerlein K, Ruth P, Westermann B, Löhr S, Schipp R. Hemocyanin and the branchial
747 heart complex of *Sepia officinalis*: are the hemocytes involved in hemocyanin
748 metabolism of coleoid cephalopods? Cell Tissue Res 2002;310:373–81.

749 [111] Alpuche J, Pereyra A, Mendoza-Hernández G, Agundis C, Rosas C, Zenteno E.
750 Purification and partial characterization of an agglutinin from *Octopus maya* serum.
751 Comp Biochem Physiol Part B Biochem & Mol Biol 2010;156:1–5.

752 [112] D'Aniello A, Strazzullo L, D'Onofrio G, Pischetola M. Electrolytes and nitrogen
753 compounds of body fluids and tissues of *Octopus vulgaris* Lam. J Comp Physiol B
754 1986;156:503–9.

755 [113] Ghiretti F. Molluscan hemocyanins. In: Wilburg KM, Young CM, editors. Physiol.
756 Mollusca. Vol. II, London, New York: Academic press; 1966, p. 233–48.

757 [114] Mangold K, Bidder AM. Appareils respiratoire et circulatoire : respiration et
758 circulation. Trait. Zool. Anat. systématique, Biol. Céphalopodes, tome V, Paris:
759 Grassé, Pierre-Paul; 1989, p. 387–434.

760 [115] Ballarin L, Cima F, Sabbadin A. Phagocytosis in the colonial ascidian *Botryllus*
761 *schlosseri*. Dev & Comp Immunol 1994;18:467–81.

762 [116] Grimaldi AM, Belcari P, Pagano E, Cacialli F, Locatello L. Immune responses of
763 *Octopus vulgaris* (Mollusca: Cephalopoda) exposed to titanium dioxide nanoparticles.
764 J Exp Mar Bio Ecol 2013;447:123–7.

765

Table

Table 1: Reported circulant Hc concentrations (mean ± SD and range, $\times 10^6$ cell ml^{-1}) in cephalopod, gastropod and bivalve mollusks

Species	*N*	Concentration	Range	Authors
Cephalopod				
Loliginidae				
Sepioteuthis lessoniana	18	2.80 ± *4.24*	-	[63]
Sepiidae				
Sepia officinalis	31	7.23 ± 5.62	0.92 - 20.31	Present study
Sepiolidae				
Euprymna scolopes	-	5.0	-	[42,64]
Octopodidae				
Eledone cirrhosa	≥ 5	> 10.0	-	[65,66]
Octopus vulgaris	28	10.67 ± 7.32	2.3 - 25.0	[40]
O. vulgaris	92	10.3 ± *7.77*	0.49 - 32.0	[62]
Gastropod				
Ampullariidae				
Pomacea canaliculata	3	1.1 ± 0.1	-	[20]
Haliotididae				
Haliotis discus discus	38	2.24	-	[18]
Planorbidae				
Biomphalaria tenagophila	10	0.25 ± 0.13	0.11 - 0.55	[19]
Turbinidae				
Turbo cornutus	35	1.50	-	[18]
Bivalve				
Cardiidae				
Cerastoderma edule	10	4.54 ± *2.21*	-	[67]
Cerastoderma glaucum	10	0.55 ± 0.22	-	[9]
Mytilidae				
Mytilus edulis	10	5.68 ± *3.63*	-	[67]
Perna perna	60	3.41 ± 1.77	-	[68]
Perna viridis	20	1.30 ± *0.35*	0.73 - 2.20	[12]
P. viridis	6	5.54 ± 1.30	-	[7]
Ostreidae				
Crassostrea ariakensis	15	0.71 ± 0.22	0.33 - 1.23	[11]
Crassostrea virginica	-	-	0.65 - 2.80	[69]
Pectinidae				
Argopecten irradians	≥ 20	37.9	-	[70]
Pharidae				
Ensis siliqua	10	6.48 ± *2.50*	-	[67]
Semelidae				
Scrobicularia plana	≥ 10	2.99	-	[6]
Tridacnidae				
Tridacna crocea	6	-	0.3 - 2.6	[71]
Unionidae				
Cristaria plicata	30	2.37 ± 0.51	-	[72]
Veneridae				
Chamelea gallina	120	-	1.2 - 2.4	[73]
Macrocallista nimbosa	51	1.08 ± *0.47*	0.12 - 2.06	[58]
M. nimbosa	40	0.99 ± *0.52*	0.26 - 2.2	[74]

In italic: data calculated from standard-error or 95% confident interval.

Table 2: Specific activity repartition in hemolymph compartments: Hcs (10×10^6 cell ml^{-1}) and plasma. Asterisk (*) indicates significance between PO- and APO-like activities in each compartment ($p<0.05$)

Specific activity	*N*	Hemolymph compartment	
		Hc	Plasma
Acid phosphatases (U mg $prot^{-1}$)	9	23.5 ± 10.6	0.1 ± 0.1
Lysozymes (µg HEW lysozyme eq. mg $prot^{-1}$)	10	21.9 ± 9.0	0.1 ± 0.1
PIs (trypsin inhibition %age)	9	0.0	31.8 ± 14.6
PO-like (U mg $prot^{-1}$)	10	20.3 ± 9.5	2.6 ± 1.0
APO-like (U mg $prot^{-1}$)		30.5 ± 7.4*	2.9 ± 0.9

Figure

Figure 1: Freshly adhesive *Sepia officinalis* Hcs presenting refringent (arrowhead) and non-refringent (arrow) granules. Inset: Hcs completely spread

Figure 2: Stained *S. officinalis* freshly adhesive Hcs; (A) Wright staining highlighting large nucleus (n), slightly basophilic cytoplasm, acidophilic granules (arrow) and lucent granules (arrowhead) in spread hemocytes; (B) Neutral red uptake staining of two Hcs highlighting lysosomal system.

Figure 3: Electron micrographs of *S. officinalis* circulating Hcs. (A) SEM micrograph of several Hcs showing similar aspect; (B) SEM micrograph of one hemocyte producing many pseudopodia; (C) Transmission electron micrograph of circulating Hcs presenting caracteristic lobate-nucleus (N) with highly condensed chromatin along the inner surface of the nuclear membrane, well-developped rough endosplasmic reticulum (rER), electron-dense lysosomal vesicles (arrow) and electron-lucent vesicles (arrowhead). Bar: 1 µm. Inset: high magnification of mitochondria (m) and Golgi apparatus (G). Bar: 0.1 µm; (D) Transmission electron micrograph of circulating Hcs presenting numerous vesicles; electron-dense lysosomal granules (arrow) and electron-lucent vesicles (arrowhead). Bar: 0.5 µm. (E-F) Electron-lucent vesicles showing inner Hcy-like molecules (small arrow). Bars: 100 nm.

Figure 4: Flow cytometer bivariate plots showing distributions of particle size (FSC) *vs* internal complexity (SSC) of fresh Hcs of *S. officinalis*. Insets representing histogram of both variables. (A) Typical cuttlefish dot-plot; (B) Dot-plot showing wide internal complexity (SSC) distribution sometimes observed.

Figure 5: Graphs representing evolution of phagocytic parameters function of time (30, 60, 120 and 180 min) at three temperatures (4, 15 and 25°C) (N = 5); (A) Phagocytic Hc percentages and (B) engulfed bead number.

Figure 6: TEM micrographs of *S. officinalis* Hc. (A) Phagocytic Hc presenting several engulfed 1 µm latex beads (b). Bar: 1 µm. Sequential events of the internalization of beads (B-D); (B) Hc-bead adhesion. Bar: 0.1 µm; (C) bead engulfment. Bar: 0.2 µm; (D) and fusion between phagosomal and lysosomal compartments. Bar: 0.5 µm.

Figure 7: Graph representing phagocytic Hc percentage and mean engulfed bead number of *S. officinalis* Hcs ($N \geq 4$; 2h incubation at 15°C) function of plasma concentration (%) treatments. Statistically significant differences were made against control (0% plasma concentration) at each plasma concentration for phagocytic cell percentage (º) and engulfed bead number (*); * and º $p<0.05$; ** $p<0.01$.

Figure 8: TEM micrographs of 1 µm latex beads (b). (A) One bead after incubation in medium without plasma add; (B) one bead after incubation in plasma presenting important Hcy-coating (arrow). Bars: 100 nm. (C) Apparent Hcy-like molecule implication in bead aggregation (arrow). Bar: 200 nm.

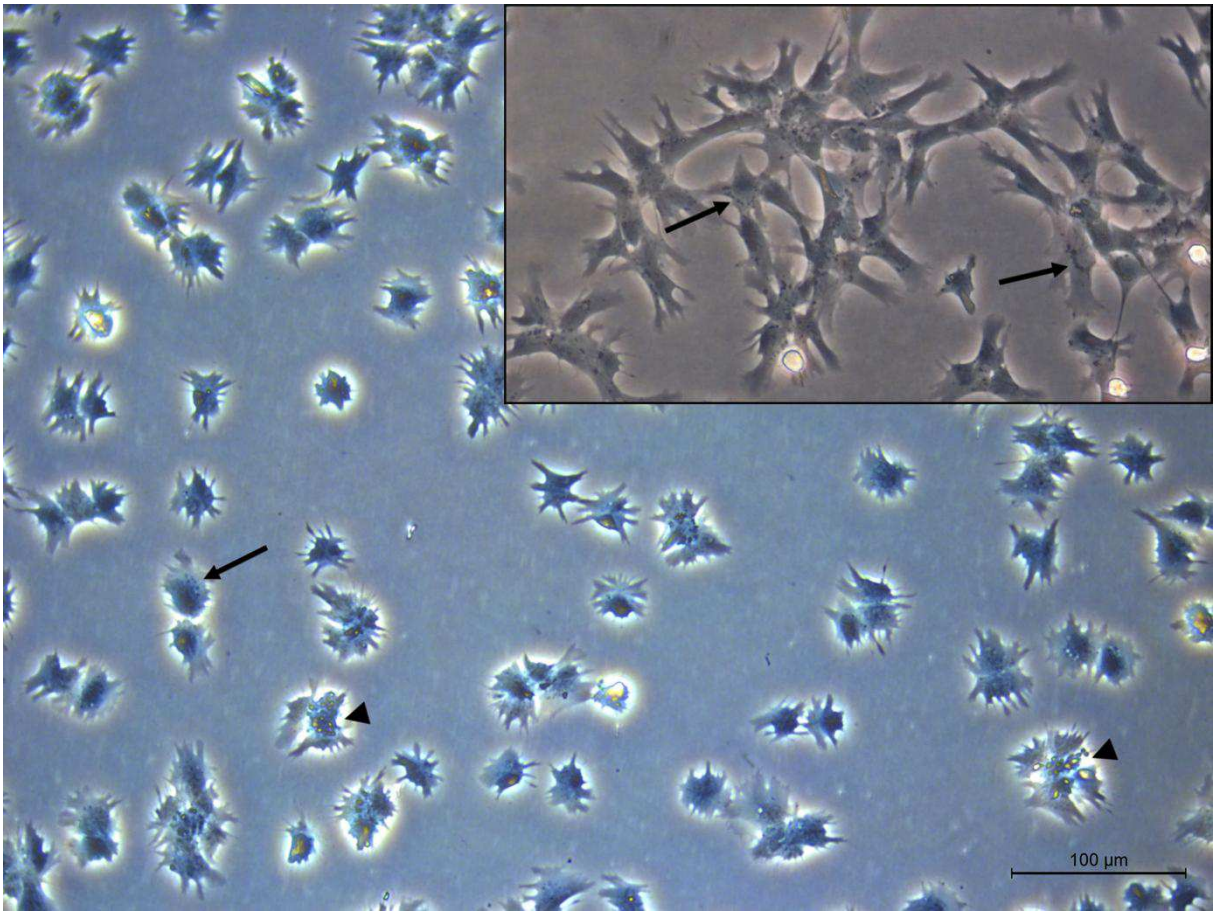

Figure 1

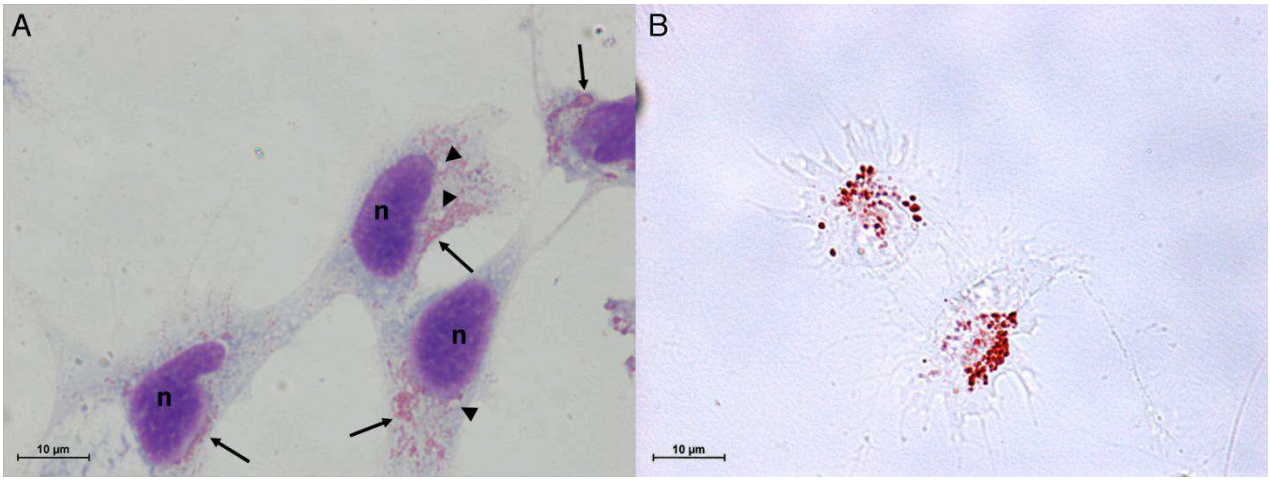

Figure 2

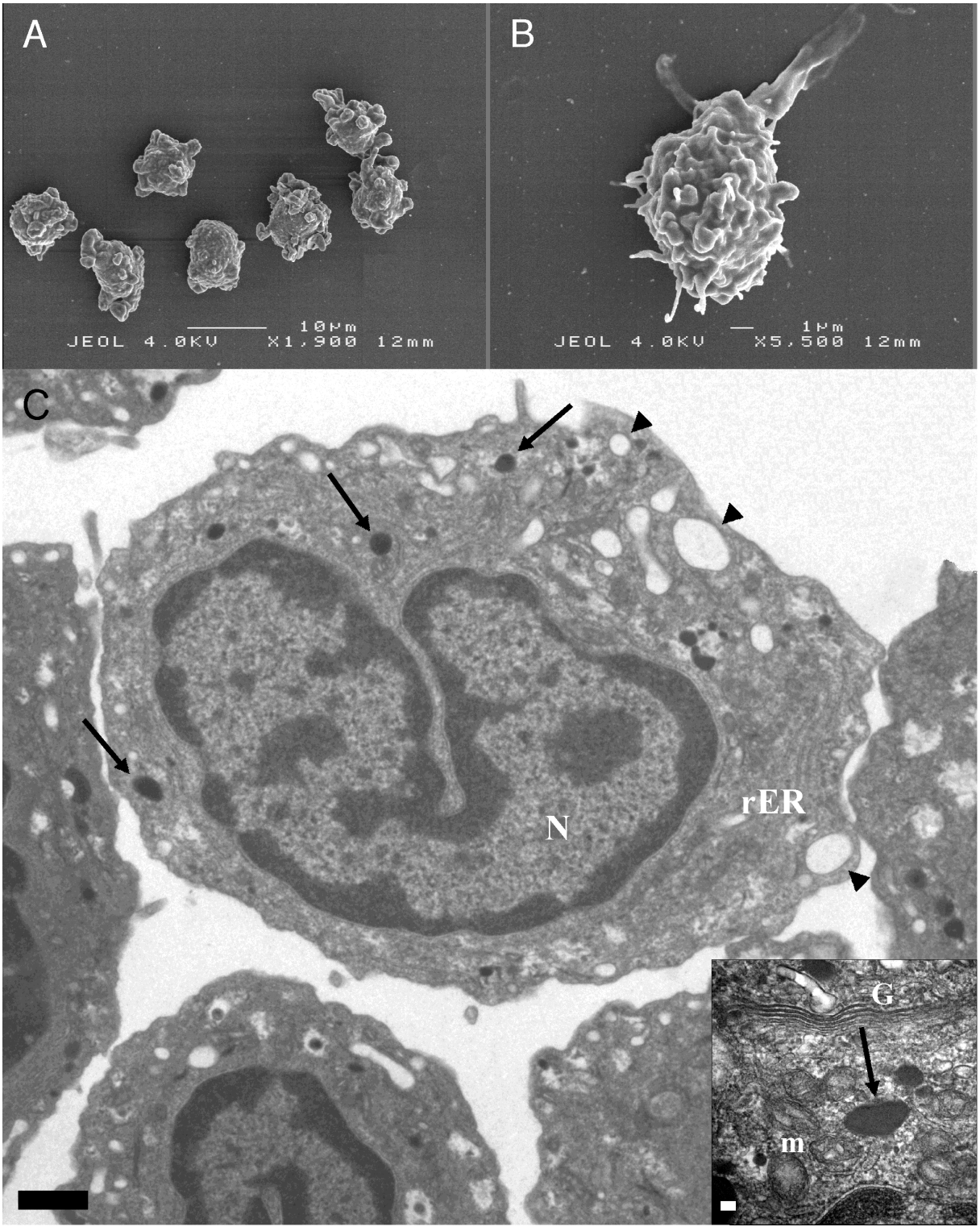
A
10µm
JEOL 4.0KV X1,900 12mm
B
1µm
JEOL 4.0KV X5,500 12mm
C
N
rER
G
m

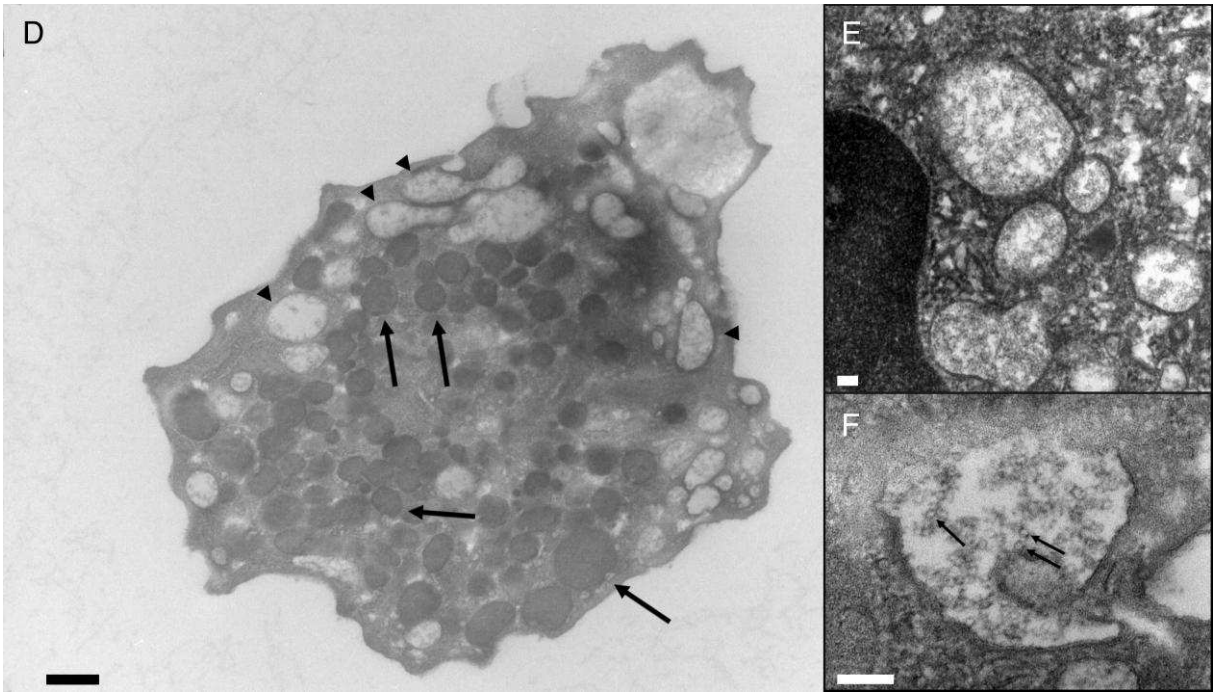

Figure 3

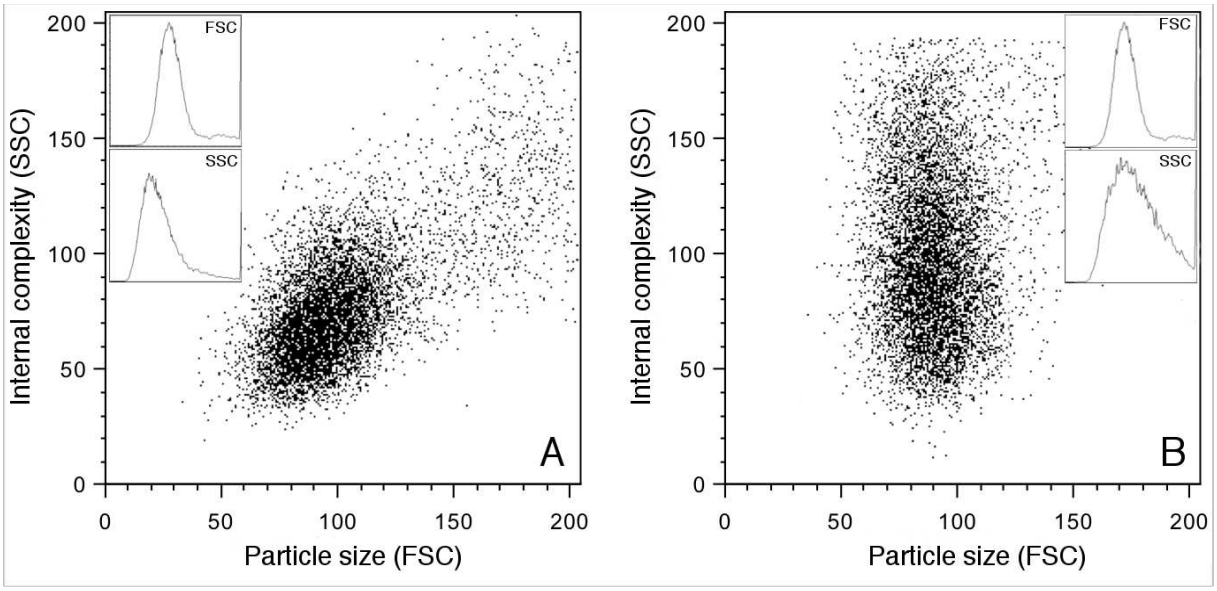

Figure 4

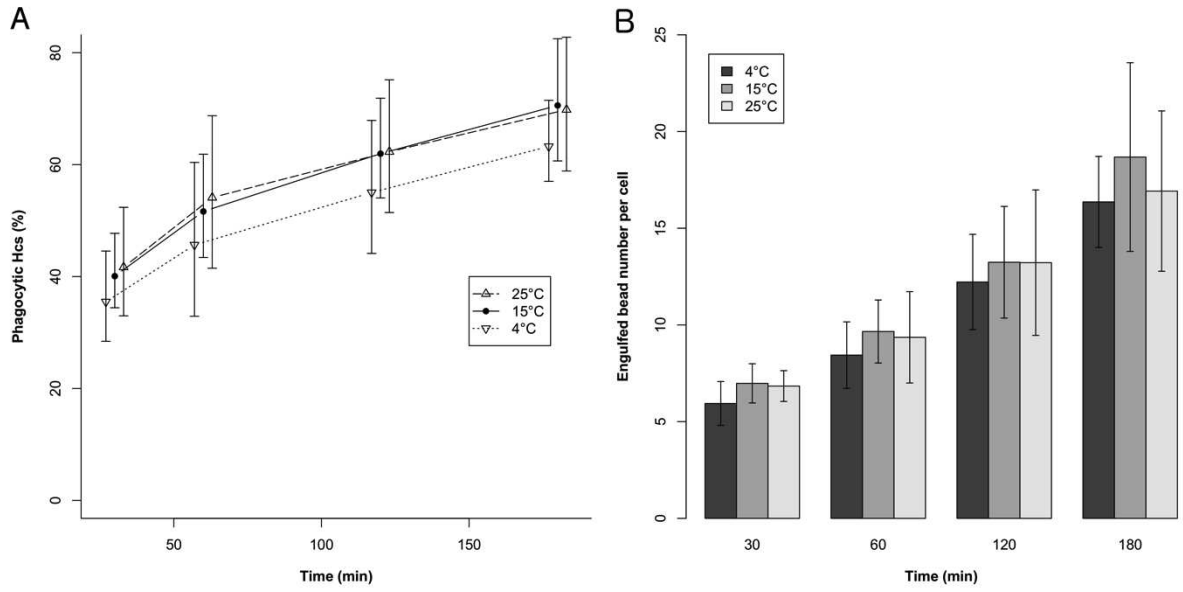

Figure 5

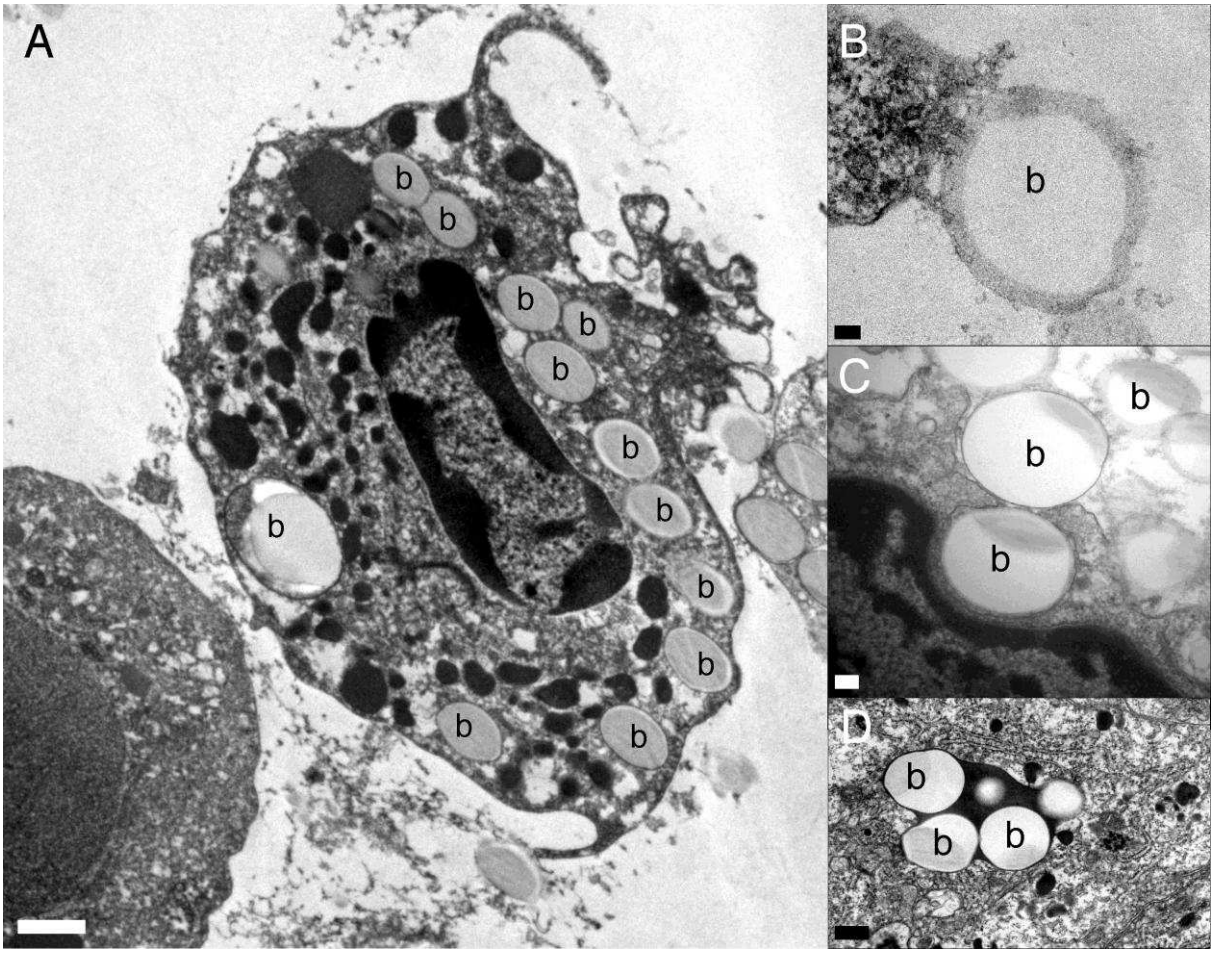

Figure 6

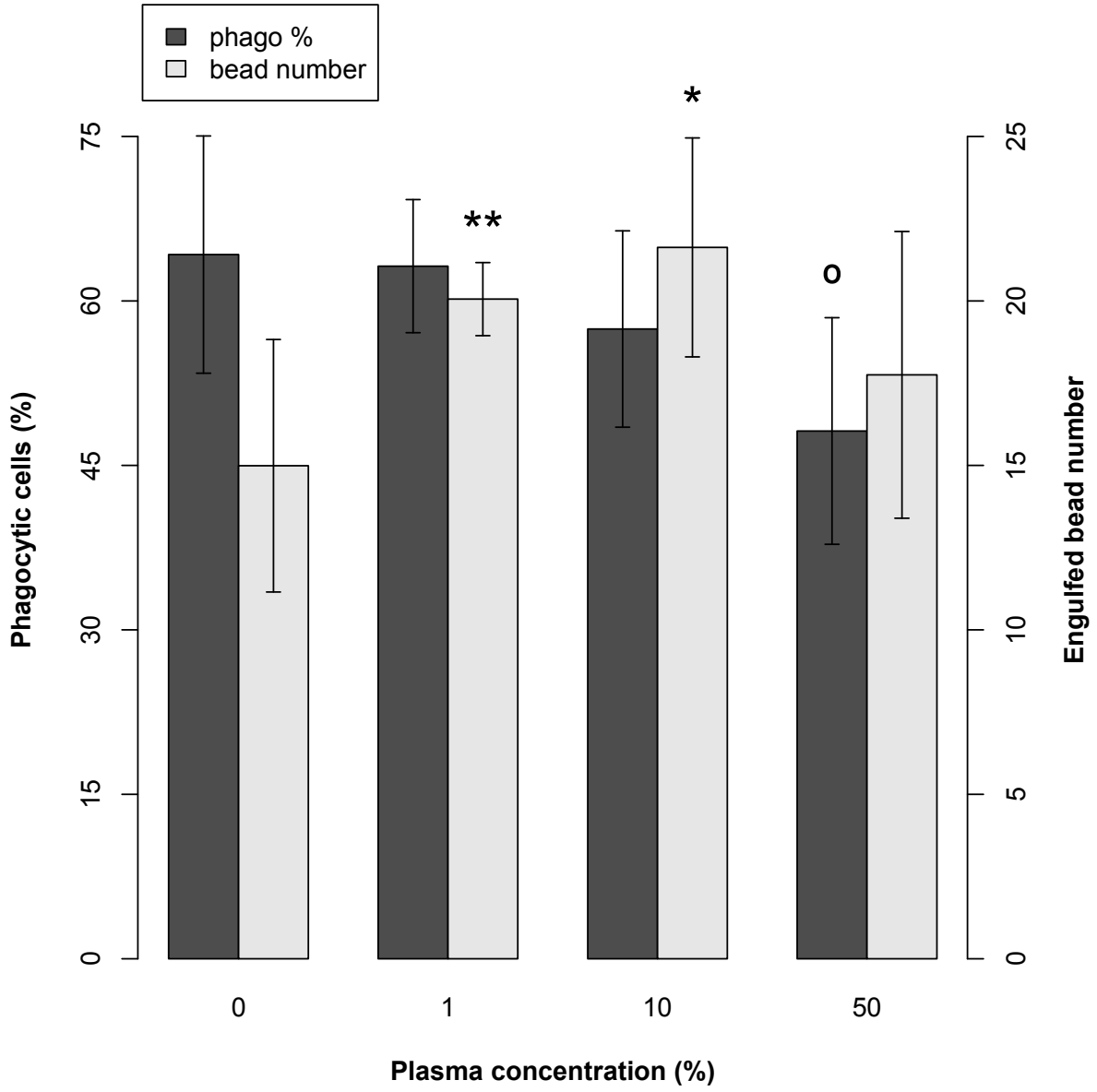
phago %
bead number
Phagocytic cells (%)
Engulfed bead number
0
15
30
45
60
75
0
5
10
15
20
25
**
*
o
0
1
10
50
Plasma concentration (%)

Figure 7

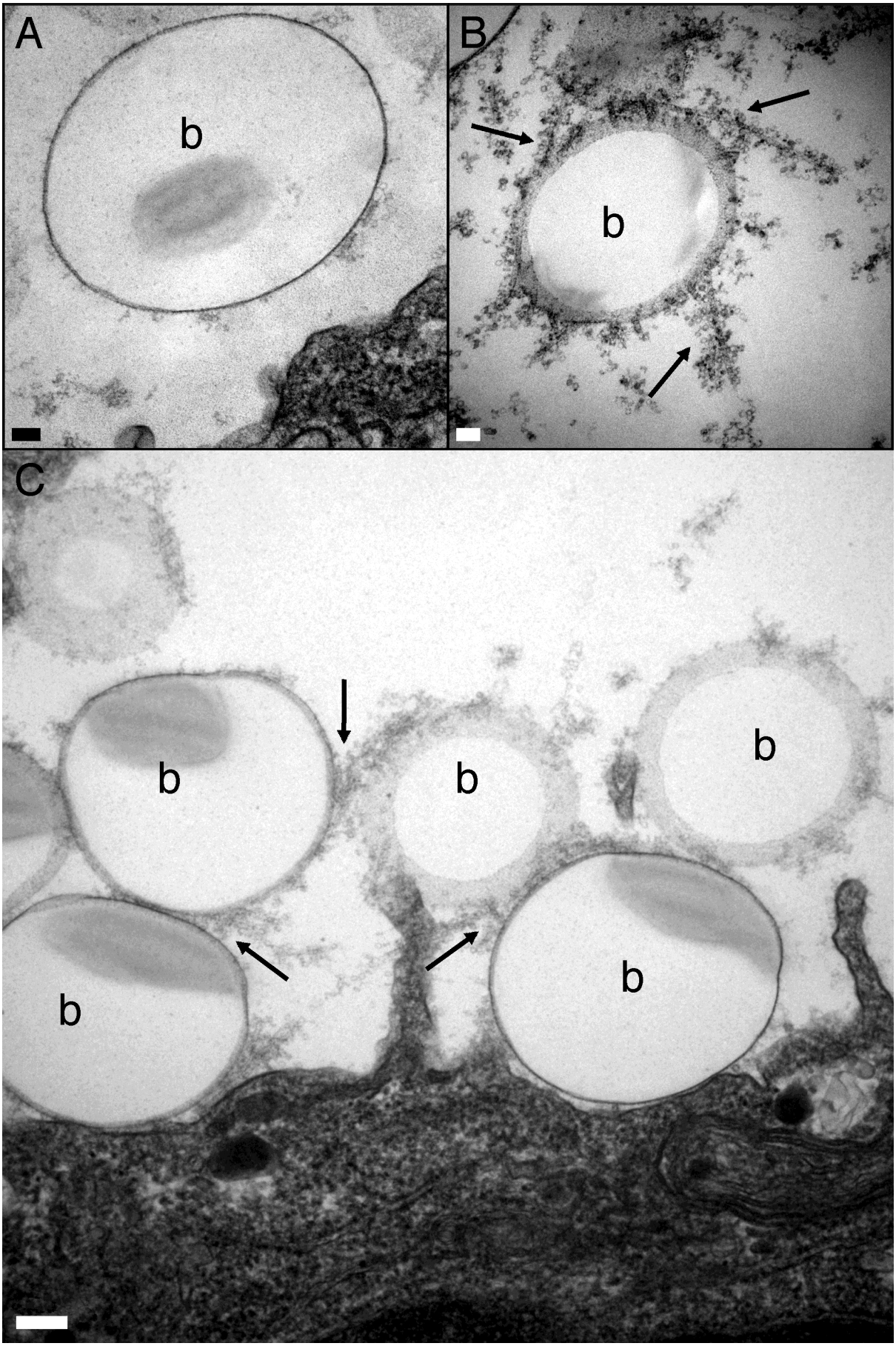

Figure 8